GIS ANALYSIS OF THE EFFECTS OF FOREST BIOMASS ON GAMMA-RADIOMETRIC IMAGES

SJ Aspin and PN Bierwirth
Australian Geological Survey Organisation

Abstract

This work relates to the interpretation of a geophysical survey in the Tumut area in New South Wales and has important implications for gamma-radiometrics interpretation in other areas. The study uses GIS layers (forest types, forest age, geology and elevation data) and Arc/Info functions to determine the gamma-ray responses for a unique forest type and age class. The use of the GIS was essential for 1) the analysis of spatial vector and raster data and 2) collecting statistics on large amounts of data. To reduce the variation due to gamma-ray source materials, specific geology and landscape parameters were also used to segregate the data. Only areas designated as granite bedrock were used and these areas were further subdivided into classes based on 1) values of slope and 2) the results of an algorithm designed to remove the attenuating materials. In pine areas, old forests reduce the gamma response by 13.5-20%. In native forest, Landsat TM was used to mask cleared areas versus dense forest for statistical analysis. In these areas, gamma-rays were reduced by 14.1-21.9%. The increase in gamma attenuation relative to pines is thought to be due to the nature of leaf litter in native forests. Results can be used to calculate relative attenuation coefficients which are compared with theoretical values. The study shows that a GIS can be a powerful tool for deriving information from the analysis of multi-layer spatial data sets.

Introduction

Airborne gamma-ray spectrometry (AGS) has been used for many years to measure the natural radioactivity of potassium, thorium and uranium, or rather the gamma-emitting isotopes in their decay series. The gamma radiation can only travel limited distances through both the air and soil or rock due to it's extremely short wavelength. These are in the range of 100m and 1m respectively (Griffiths & King, 1981). Airborne or hand held spectrometers measure the absorption of a γ ray photon by the emission of a flash of visible light. The scintillation is converted into an electrical pulse by a photomultiplier device. Although a range of energies are recorded, it is still common practice that only the energy windows for potassium (K), thorium (Th), uranium (U) and total count (TC) are used. Table 1 shows the typical data channels for an acquisition system.

Table 1. Data channels for an airborne gamma survey.

Channel/Element analysed	Isotope sensed	Gamma-ray energy (MeV)	Wavelength (nanometres)	Energy Window (MeV)
1. Potassium	40K	1.46	$8.50 * 10^{-4}$	1.37 - 1.57
2. Uranium	214Bi	1.76	$7.05 * 10^{-4}$	1.66 - 1.86
3. Thorium	208Th	2.62	$4.74 * 10^{-4}$	2.41 - 2.81
4. Total Count				0.40 - 3.00

Little practical research appears to have been done on the effects of vegetation on airborne gamma ray measurements. One study was performed by Glynn et al. (1988) looking at the problems arising from gamma ray measurements taken over forests covered in deep snow. Another (Kogan et al., 1969) reports that up to 15% of the potassium signal reaching the sensor comes from the biomass. Lavreau et al. (1991) recognise that moisture and dense vegetation effectively screen airborne data and this needs to be considered in the processing sequence.

Lavreau et al. go on further to say that satellite imagery can be of assistance by using it to calculate water/vegetation index images and using this to then correct the gamma data.

A helicopter survey over the Bago-Maragle region of NSW (Figure 1) in February 1996 resulted in a high quality AGS data set. The survey was flown at 80m and the spacing between flight lines was 200m. The region consists of steep hills with highland plains and is extensively covered with both native forests and pine plantations - some of a historical nature. In Bago-Maragle the State Forests of New South Wales (SFNSW) has plantations of radiata pine ranging from 1922 up to 1996 for the year they were planted in. SFNSW also produced the forest age class GIS coverage that was used in this study. The object of this study is to attempt to measure the impact that vegetation biomass, in particular radiata pine and native forest, predominantly eucalypt, has on gamma ray data collected by airborne methods. An estimation of how much the vegetation affects the signal may be used in future surveys to assist in interpretation and potentially correct the data. For this forum, another aim was to demonstrate the versatility of the GIS for analysing multi-layer information.

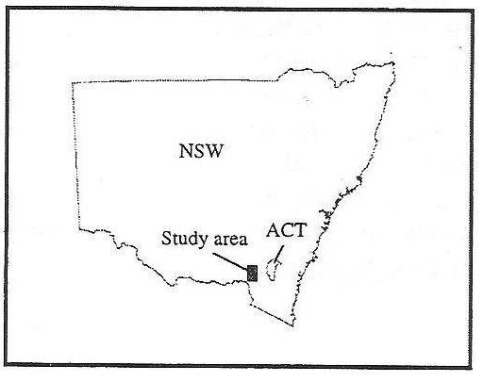

Figure 1. Location of the study area.

Methods

The data used for this survey consisted of four bands of airborne collected radiometric data; potassium (K), thorium (Th), uranium (U) and total count (TC), and an arc/info forestry coverage that includes both the species type and year that the plantations were planted. These layers were imported into both Ermapper and Arc/Info as required, usually using the arc commands either *gridfloat* or *floatgrid* depending on the initial format of the data.

To reduce variations in the data to be used, many sources of potential interference or variance were removed. This included only using data that was collected over the Green Hills Granite (includes New Maragle Granite) as identified on the Wagga Wagga 1:250,000 metallogenic map (Degeling, 1977). Likewise, only data that was covered by radiata pine with known planting dates were used.

An initial problem with the project became apparent due to the lack of a digital geology coverage covering the Bago region. The only map available was the Wagga Wagga 1:250,000 metallogenic map and this was not considered detailed enough to accurately identify granitic geology in the area. The problem was solved by using the K and magnetics images to define the granite/basalt boundary. Basalt has a low K value and a relatively high magnetics value compared to the surrounding granite. Areas containing geology other than granite or basalt were grouped in the northwest and south of the survey area so were also relatively easy to identify. Areas where non-granitic geology occurred were assigned a null value.

Layers imported into GRID included;

- granite mask (edited K image)

- radiata pine year of planting coverage - a layer that shows where radiata pines occur in the Bago region and in what year they were planted.
- K, U, Th, TC - 4 separate gamma radiometric layers that cover the Bago study region.
- DEM - Digital Elevation Model.

The granite mask was then imported into Arc/Info GRID and used to mask out all non-granitic areas on the 4 gamma data sets. This was performed by using a series of *con* and *setnull* statements in GRID. For example; *new_grid1 = con(mask, k_grid, -9999)* and then *new_grid2 = setnull(new_grid1 == -9999, new_grid1)*. A similar process using the radiata coverage was then used to mask out non radiata pine areas.

Classification by slope

To reduce the influence of soil variation in the various age classes two methods of dividing the data into classes were considered:

- percentage of slope
- mathematical removal of screening effects (attenuation modelling).

These are discussed in further detail below.

To produce the percentage-of-slope grids the *slope* function in GRID was applied to the DEM to create a grid representing percentage of slope for example; *slope_grid = slope(dem_in, percentrise*. The new grid was then used in conditional (*con*) statements to create 3 slope categories. They are: slope $\leq$ 10%, 10% < slope $\leq$ 20% and 20% < slope $\leq$ 30%. Values outside of these gates were assigned a null value using the function *setnull* in GRID as outlined above. Other slope classes were considered, for example, Soil Conservation Agency of NSW classifications (McDonald et al., 1990). Their classes appear more suited to flatter terrain than the steep terrain of the Bago/Maragle region. The *con* and *setnull* functions in GRID were then used to create further grids that contained K, U, Th and TC values only where granite and radiata pines occur.

The GRID function *zonalstats* was then used to classify these newly created gamma data grids according to the year in which the radiata pines covering the area were planted. The mean was calculated using the *zonalstats moment* option. For example; k_stats = zonalstats(age_grid, k_grid, moment). The result was a table in INFO that listed the year planted, mean gamma ray count for that year, standard deviation and number of values (or pixels overlain by a particular section of the coverage) for that year. All of the tables were then imported to a spreadsheet.

Attenuation modelling

This is a method developed for removing attenuation effects in multiband imagery. The technique applied to gamma-ray data (Bierwirth, 1994) was adapted from work originally aimed at removing water depth effects from optical remote sensing imagery (Bierwirth et al, 1993). The idea was that an image could be derived where attenuation (ie. vegetation) effects were largely removed and variations in parent materials remained. This image then could be used to reduce the "noise" associated with geological and soil factors.

The absorption of gamma-ray photons by an attenuating medium is given by:

$$I_{ri} = I_{0i}\, e^{-u_i r} \qquad (1)$$

where I_{0i} is the intensity of gamma-rays emanating from a covered source in wavelength i and I_{ri} is the intensity after a distance r has been traversed through material with a linear absorption coefficient, u. By averaging over all wavelengths available, the depth of attenuating cover, r, can be represented by:

$$r = \sum_{i=1}^{N} \frac{\ln I_{ri}}{-u_i N} - \sum_{i=1}^{N} \frac{\ln I_{0i}}{-u_i N} \qquad (2)$$

where N is the number of wavelengths. The second term is set to a constant, zero in fact. This is roughly equivalent to assuming that the average intensity of radiation sources is the same and that variations in the amplitude of the spectrum is due to attenuating cover. The derived attenuating thickness (r) can be calculated using band values (I_{ri}) and attenuation coefficients (u_i) derived for the appropriate density (Grasty, 1979). The value for overburden depth can then be substituted into equation 1 to derive the source intensity (I_{0i}) for each element and effectively remove attenuation effects. For example, the area of the K image before and after application of the algorithm is shown in Figure 2.

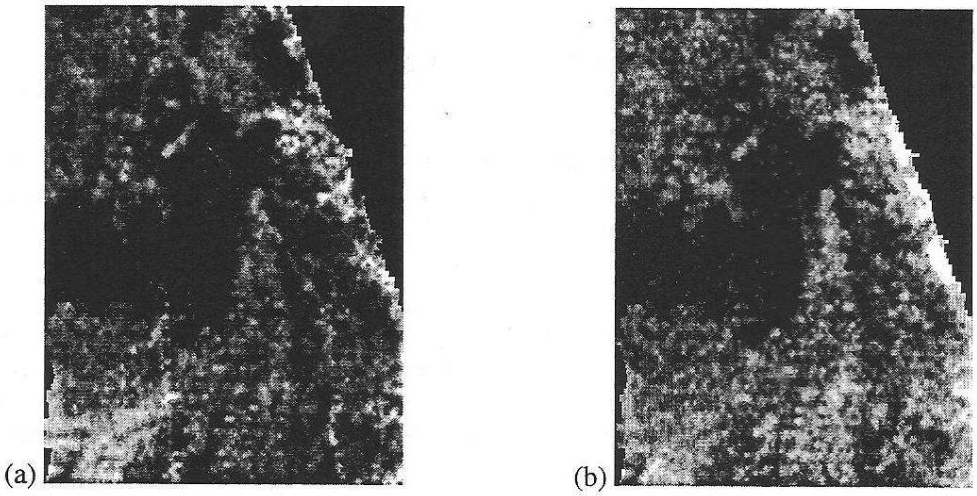

Figure 2. Airborne K data before and after attenuation modelling. The powerlines (pale linear features) that are visible in (a) are not visible in (b) due to the effects of the surrounding vegetation having been removed.

The data set produced by the attenuation modelling was used to create 4 divisions of the gamma data according to how much it had been attenuated during the modelling stage. The *con*, *setnull* and *zonalstats* functions were used in GRID to produce a spreadsheet of the mean gamma data classified according to the attenuated values and the radiata pine year of planting.

The data in the spreadsheets were further edited. This consisted of removing data prior to 1960. Data prior to 1960 was removed because radiata pine trees are normally harvested after 25 - 30 years (pers. comm. Bob Gay SFNSW) and also because the data was relatively sparse in the number of counts in age classes prior to 1960. Analysis was also performed on the gamma ray data where a powerline clearing goes through native forest. Mean values were determined for powerline areas and adjacent forest. Results of this analysis are presented later.

Results and analysis

Line graphs were created to give a visual representation of the year of planting versus the gamma ray signal for unclassified slope (Fig 3a-d) and attenuation ratio classes (Fig 4a-c).

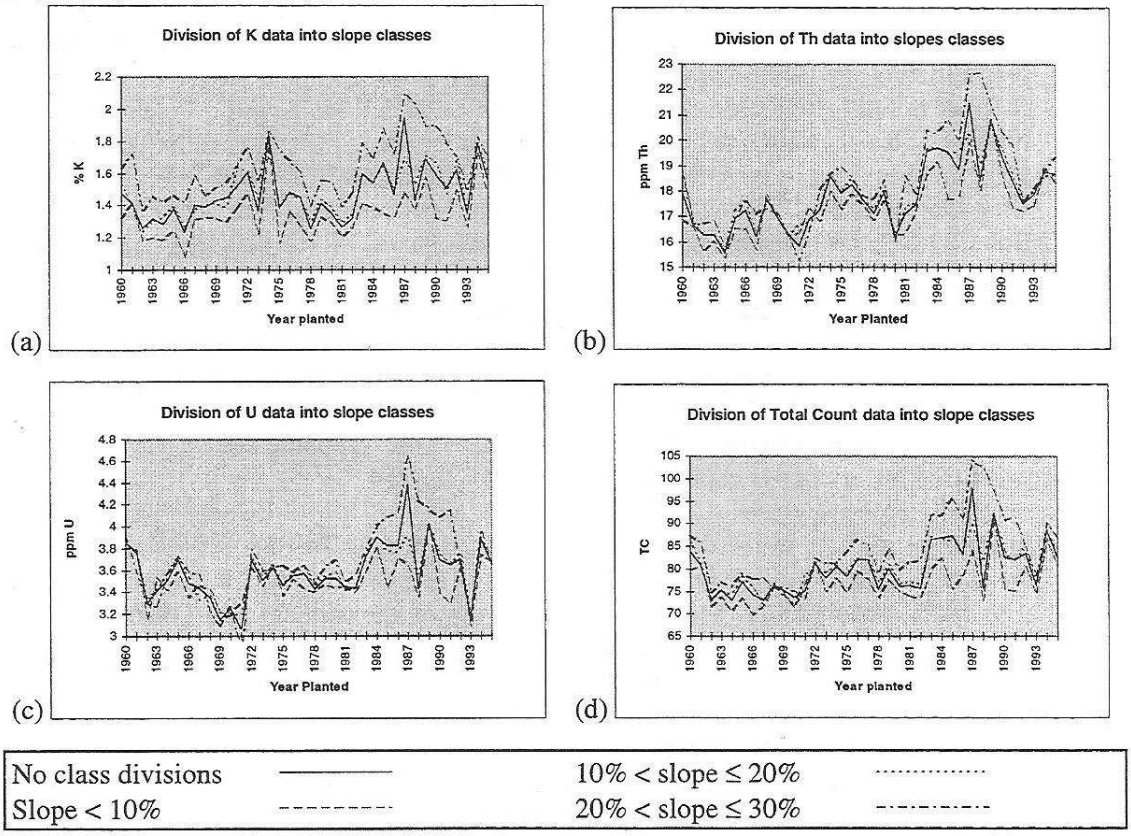

Figure 3. Mean gamma-element concentrations for vegetation age class and various slope classes (a) K (b) Th (c) U (d) total count.

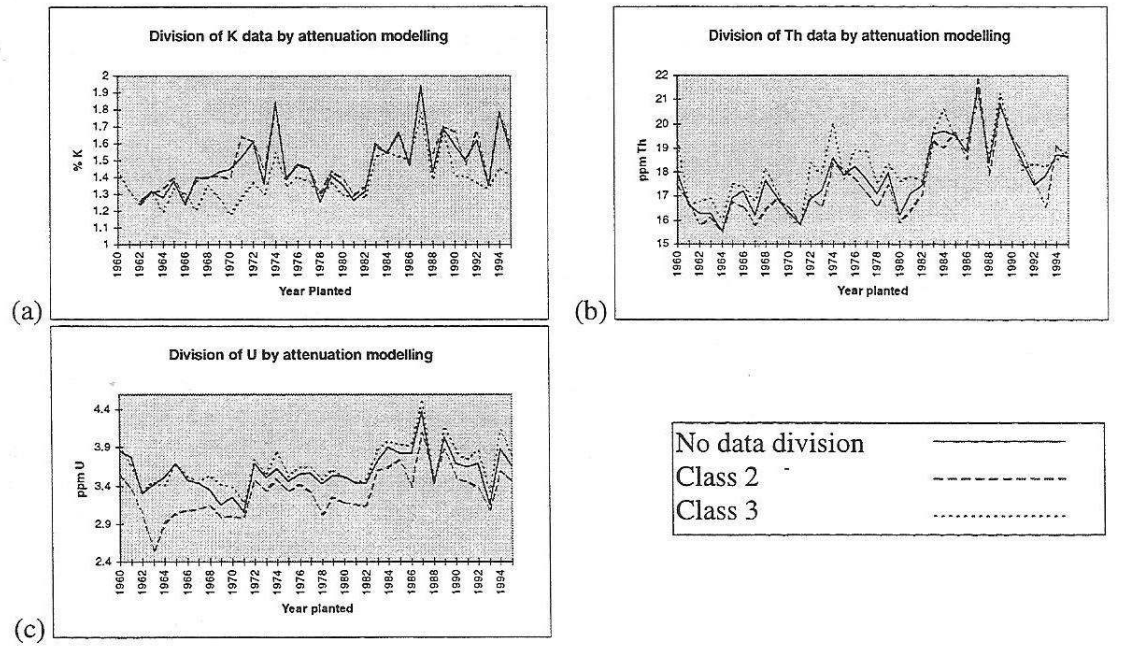

Figure 4. Gamma data, K (a), Th (b) and U (c), plotted for classes defined by data ranges in corrected (by attenuation modelling) K, Th and U images. Only classes 2 and 3 of 4 classes are shown here because classes 1 and 4 are open ended and subject to low and high extremes of data respectively.

Discussion

All the graphs (Figures 3a-d) showed a general increase in the gamma ray value from 1960 to 1995. There is also however numerous high and low values throughout that time period. Explanations may be offered for the occurrence of some of these peaks and troughs. The data peaks at 1987 then drops off again. The reason for this maybe the change in the method of preparation of the land before planting new trees from clearing the ground to a technique called chopper rolling where old vegetation is pushed aside and the new trees planted in the cleared furrows. This vegetation debris may attenuate gamma-rays. Chopper rolling commenced in the early nineties (pers. comm. Bob Gay SFNSW). Variations in the data may also have occurred after approximately 1978 because of the replanting of previously harvested areas (pers. comm. Bob Gay SFNSW) in some but not all of the age classes. Some pine tree remnants would still be in the area when new pines were planted for the second time in that area, therefore blocking the gamma rays that were recorded by the aircraft.

As well as the above changes in forest practise, a significant component of the "noise" is due to regolith variations. In figure 3, the slope class divisions highlight that steeper slopes generally have higher concentrations for all elements. This supports the interpretation that less weathered mineralogy is exposed in the incised valleys.

In figure 4, the classes of data based on attenuation modelling should theoretically represent areas of similar regolith type. This should have reduced the regolith "noise". It has worked well for K reducing high K areas in the 1970 - 1974 age classes. For Th and U there is little change probably because these elements are less variable in concentration as they are more resistant to weathering being sourced from accessory minerals in the granite.

The slope of the regression lines for selected graphs may be used to work out relative attenuation and the percentage of the gamma-ray signal the pine trees are blocking for different elements. For K data, class 3 of figure 4(a) had the best linear correlation. For both Th and U the original graphs (solid lines) were used.

Deriving relative vegetation attenuation-coefficients

Assuming that no attenuation of gamma-rays due to vegetation occurs in the newly planted areas, the graphs showing age class versus element concentration together with equation 1, can be used to calculate the ratios of attenuation between elements. For example:

$u_k/u_{Th} = \ln(k_1/k_2)/\ln(Th_1/Th_2)$

where k_1 = potassium gamma-ray counts for the oldest forest
k_2 = potassium gamma-ray counts for cleared land
u_k and u_{Th} = attenuation coefficients for K and Th respectively.

Table 2 shows the relative attenuation of gamma-rays of the different energies corresponding to the gamma-emitting elements. For both types of forest the ratios are similar to theoretical values, although potassium attenuation is larger than expected relative to Th and U. This is the reverse of what would be expected if there was a component of K in the vegetation as found by Kogan et al (1969).

Table 2. Relative attenuation coefficients

	u_k/u_{Th}	u_{Th}/u_u	u_u/u_k
Pine Forest	1.48	1.05	0.65
Native Forest	1.63	0.85	0.72
Theoretical-1	1.34	0.82	0.91

Table 3 gives the results of gamma signal reduction from cleared land to dense forest. This is highly significant information for the interpretation of gamma-element images particularly when subtle variations in ground concentrations overlap with variable vegetation density. The slightly higher values for native forest is thought to be due to thicker, wetter leaf litter.

Table 3. Percent reduction of gamma-ray counts

	K	Th	U
Pine Forest	20.0	14.0	13.5
Native Forest	21.9	14.1	16.4

Conclusions

The reduction in counts of airborne gamma-ray data is significant ranging from 13.5% to 20% for radiata pine forests and from 14.1% to 21.9% for native forests in the Bago-Maragle area. In surveys flown over forested areas this has important implications for the interpretation of gamma ray data as subtle variations may be misinterpreted because of the variable screening effects of vegetation biomass.

This study has demonstrated that GIS is a powerful tool to perform statistical analysis on large quantities of multi-layer data.

Acknowledgments

We wish to thank Philip Ryan at CSIRO forestry for providing a spreadsheet of field data and general comments throughout our discussions with him. The authors are grateful to State Forests of New South Wales for providing the GIS coverage of forest data, and to Bob Gay for providing comments. Andrew Loughead at CSIRO forestry is also gratefully acknowledged for providing the DEM.

References

Bierwirth, P.N., Lee, T., Burne, R.V. (1993) Shallow sea-floor reflectance and water depth derived by unmixing multispectral imagery. Photogrammetric Engineering and Remote Sensing, 59, (3), pp331-338.

Bierwirth P.N. (1994). Image processing of airborne gamma-ray data for soils information - Wagga Wagga, NSW, 7th Australasian Remote Sensing Conference Proceedings, Melbourne.

Degeling P.R. (1977). Wagga Wagga 1:250 000 metallogenic map, Geol. Surv. NSW, Sydney.

Glynn J.E., Carroll T.R., Holman P.B. and Grasty R.L. (1988) An airborne gamma ray snow survey of a forest covered area with a deep snowpack, Remote Sensing of Environment, 26, pp149 - 160.

Grasty R.L. (1979). Gamma ray spectrometric methods in uranium exploration - theory and operational procedures, in Geophysics and Geochemistry in the Search for Metallic Ores; Geological Survey of Canada, Economic Geology Report 31.

Griffiths D.H. and King R.F. (1981). Applied geophysics for geologists and engineers, Pergamon Press, Australia.

Kogan R.M., Nazarov I.M. and Fridman Sh.D. (1971). Gamma spectrometry of natural environments and formations, Israel Program for Scientific Translations, pp 124 - 132.

Lavreau J. and Fernandez-Alonso M. (1991). Correcting airborne radiometric data for water/vegetation screening using Landsat thematic mapper imagery, Eighth Thematic Conference on Geologic Remote Sensing, Denver, Colorado, USA.

McDonald R.C., Isbell R.F., Speight J.G., Walker J. And Hopkins M.S.(1990). Australian soil and land survey field handbook 2nd Edtn, Inkata Press Pty Ltd, Melbourne.